

See discussions, stats, and author profiles for this publication at: <https://www.researchgate.net/publication/231344789>

Vanadium(IV) thiolate chemistry: preparation, structure, and properties of $[\text{VE}(\text{SCH}_2\text{CH}_2\text{S})_2]_2-$ (E = O,S)

ARTICLE *in* INORGANIC CHEMISTRY · SEPTEMBER 1985

Impact Factor: 4.76 · DOI: 10.1021/ic00214a040

CITATIONS

50

READS

19

3 AUTHORS, INCLUDING:



John C Huffman

Indiana University Bloomington

1,226 PUBLICATIONS 27,060 CITATIONS

SEE PROFILE



George Christou

University of Florida

757 PUBLICATIONS 28,963 CITATIONS

SEE PROFILE

FeOH^{2+} as a reactant results in a dissociative ion-pair mechanism, in which the observed forward rate constant should be approximately $2 \times 10^3 \text{ M}^{-1} \text{ s}^{-1}$ for a ligand with zero charge (H_3PO_4) at room temperature. From Table IV the constant k_3 (at 25°C) of $\sim 9 \times 10^6 \text{ M}^{-1} \text{ s}^{-1}$ is over 3 orders of magnitude higher. Furthermore, while the activation parameters for ligand substitution should be lower than the values for water solvent exchange, ΔH^\ddagger for the reaction involving FeOH^{2+} appears to be much too low when compared to the activation parameters³³ (ΔH^\ddagger , ΔS^\ddagger) for water exchange ($15.3 \text{ kcal mol}^{-1}$ and $2.9 \text{ cal mol}^{-1} \text{ deg}^{-1}$ for Fe^{3+} , and $10.14 \text{ kcal mol}^{-1}$ and $1.26 \text{ cal mol}^{-1} \text{ deg}^{-1}$ for FeOH^{2+}). On this basis, it is proposed that the associative mechanism involving Fe^{3+} is more reasonable. Finally the mechanism of complex formation currently proposed for a number of tervalent cations, including other iron(III)-ligand substitution reactions, is based on associative interchange.³⁴

The detection of the ferric diphosphate complex, $\text{Fe}(\text{H}_2\text{PO}_4)_2^+$, demonstrated the value of using a kinetic technique for the characterization of the solution species. While various complex solute species have been postulated (Table I), $\text{Fe}(\text{H}_2\text{PO}_4)_2^+$ was never specifically identified. Under the experimental conditions that lead to the precipitation of uniform dispersions of ferric phosphate particles, significant concentrations of this complex would be present in solution.

Only a few data are found in the literature describing the kinetics of an FeL_2 complex. The observed rate constant for the ferric dichloride species was given as $324 \text{ M}^{-1} \text{ s}^{-1}$, which is ap-

proximately 15 times larger than the rate constant for the formation of the monochloro species,³⁵ and may be compared with the maximum value of $160 \text{ M}^{-1} \text{ s}^{-1}$ for $\text{Fe}(\text{H}_2\text{PO}_4)_2^+$. In this study, the rate constants for the mono- and diphosphate species showed a wider difference, the ratio being approximately 1:0.002 if a comparison between pathway 2 (Table IV) and $k(\text{maximum})$ (Table VI) is made. Clearly, the type of ligand already present in the inner coordination sphere of iron(III) has a strong influence on the rate of substitution of an additional water molecule. Out of the four parallel pathways that were considered, only two were found to contribute significantly. The activation parameters for both the mono- and diphosphate iron(III) species are listed in Tables IV and VI, and the values appear to be reasonable. As a consequence of the several rapidly established proton-transfer reactions that have to be taken into account, the relative importance of individual steps cannot be clearly assessed, in contrast to the situation with simple ligands such as Cl^- .³⁵ The formation of $\text{Fe}(\text{H}_2\text{PO}_4)_2^+$ by involving H_2PO_4^- as a reactant also tends to support the formation of the monophosphate species through an analogous pathway.

This work offers strong evidence that the static spectrophotometric procedure may not be sufficiently sensitive to detect successive complexation. In contrast, time-resolved absorbance measurements (e.g. Figure 6) provide an effective method for identification of a series of species in solution.

In conclusion, it appears that the formation of ferric phosphate complexes under these conditions can best be represented by associative mechanisms for both pH-dependent and -independent pathways, in which the hexaaquoiron(III) ion is involved. The recent study by Grant and Jordan³³ supports the view that substitution involving Fe^{3+} is associative interchange while reactions with FeOH^{2+} are dissociative in nature.

Registry No. Fe, 7439-89-6; H_3PO_4 , 7664-38-2.

- (31) (a) Eigen, M.; Wilkins, R. G. "Mechanisms of Inorganic Reactions"; American Chemical Society: Washington, DC, 1965, Adv. Chem. Ser. No. 49. (b) Wilkins, R. G. "The Study of Kinetics and Mechanism of Reactions of Transition Metal Complexes"; Allyn and Bacon: Boston, 1974. (c) Mentasti, E. *Inorg. Chem.* **1979**, *18*, 1512. (d) Bridger, K.; Patel, R. C.; Matijević, E. *Polyhedron* **1982**, *1*, 269. (e) Ishihara, K.; Funshashi, S.; Tanaka, M. *Inorg. Chem.* **1983**, *22*, 194.
- (32) Bjerrum, N.; Dahm, C. R. *Z. Phys. Chem.* **1931**, 627.
- (33) Grant, M.; Jordan, R. B. *Inorg. Chem.* **1981**, *20*, 55.
- (34) Mentasti, E.; Secco, F.; Venturini, M. *Inorg. Chem.* **1982**, *21*, 2314.

- (35) Strahm, E.; Patel, R. C.; Matijević, E. *J. Phys. Chem.* **1979**, *83*, 1689.

Contribution from the Department of Chemistry and the Molecular Structure Center, Indiana University, Bloomington, Indiana 47405

Vanadium(IV) Thiolate Chemistry: Preparation, Structure, and Properties of $[\text{VE}(\text{SCH}_2\text{CH}_2\text{S})_2]^{2-}$ (E = O, S)

JOANNA K. MONEY, JOHN C. HUFFMAN, and GEORGE CHRISTOU*

Received January 25, 1985

The synthesis, structure, and properties of vanadium(IV) complexes with the ethane-1,2-dithiolate ligand (edt^{2-}) are described. $(\text{NMe}_4)\text{Na}[\text{VO}(\text{edt})_2] \cdot 2\text{EtOH}$ crystallizes in monoclinic space group $P2_1/n$ with unit cell parameters (at ca. -159°C) $a = 21.312$ (5) Å, $b = 10.906$ (2) Å, $c = 9.381$ (1) Å, $\beta = 92.77$ (1)°, and $Z = 4$. The vanadium is in a square-pyramidal coordination geometry with the multiply bonded oxygen at the apex ($\text{V}=\text{O} = 1.625$ (2) Å) and four ligand sulfur atoms in the base. The anion, cations, and solvent molecules pack into discrete units of C_{2h} symmetry. $[\text{VO}(\text{edt})_2]^{2-}$ was cleanly converted into $[\text{VS}(\text{edt})_2]^{2-}$ with hexamethyldisilthiane, $(\text{Me}_3\text{Si})_2\text{S}$. $(\text{PPh}_4)\text{Na}[\text{VS}(\text{edt})_2] \cdot x\text{Et}_2\text{O}$ crystallizes in triclinic space group $P\bar{1}$ with unit cell parameters (at ca. -160°C) $a = 17.201$ (5) Å, $b = 10.983$ (3) Å, $c = 9.919$ (3) Å, $\alpha = 65.84$ (1)°, $\beta = 106.63$ (1)°, $\gamma = 93.32$ (2)°, and $Z = 2$. The anion is isostructural with $[\text{VO}(\text{edt})_2]^{2-}$ except for the presence of the apical sulfur ($\text{V}=\text{S} = 2.087$ (1) Å). The anion, cations, and solvent molecules again pack into discrete dimers, but of a different structure of D_{2h} symmetry. This is only the second example of a structurally characterized species containing the $\text{V}=\text{S}^{2+}$ moiety. Infrared, electrochemical, and UV/visible studies of the two complexes are described.

Introduction

Innumerable complexes of vanadium(IV) containing the vanadyl ($\text{V}=\text{O}^{2+}$) unit have been prepared and studied in detail over the years. In the solid state, such species are predominantly either square pyramidal (VOL_4 ; L = ligand), with the multiply bonded oxygen atom in the apical position,¹⁻⁴ or distorted octahedral

($\text{VOL}_4\text{L}'$), in which a sixth ligand (L') has occupied the vacant sixth position trans to the $\text{V}=\text{O}$ group.⁵⁻⁸ Other structural variants are also known, but much less common, including trigonal-bipyramidal complexes⁹ and one-dimensional polymers due

- (1) Selbin, J. *Chem. Rev.* **1965**, *65*, 153; *Coord. Chem. Rev.* **1966**, *1*, 293.
- (2) Bruins, D.; Weaver, D. L. *Inorg. Chem.* **1970**, *9*, 130.
- (3) Henrick, K.; Raston, C. L.; White, A. H. *J. Chem. Soc., Dalton Trans.* **1976**, 26.

- (4) Tapscott, R. E.; Belford, R. L.; Paul, I. C. *Inorg. Chem.* **1968**, *7*, 356.
- (5) Form, G. E.; Raper, E. S.; Oughtred, R. E.; Shearer, H. M. M. *J. Chem. Soc., Chem. Commun.* **1972**, 945.
- (6) Cotton, F. A.; Lewis, G. E.; Mott, G. N. *Inorg. Chem.* **1982**, *21*, 3127.
- (7) Wiegardt, K.; Bossek, U.; Volkmar, K.; Swiridoff, W.; Weiss, J. *Inorg. Chem.* **1984**, *23*, 1387.
- (8) Demsar, A.; Bukovec, P. *J. Fluorine Chem.* **1984**, *24*, 369.

to ($\cdots V=O\cdots V=O\cdots V=O\cdots$) chain formation.¹⁰⁻¹²

Much rarer in vanadium(IV) chemistry are complexes containing the thiovanadyl ($V=S^{2+}$) moiety. Of the handful of complexes prepared,¹³⁻¹⁶ only VS(acen) (acen = *N,N'*-ethylenebis(acetylacetonylideneaminato)) has been structurally characterized,¹⁶ confirming square-pyramidal geometry and a $V=S$ bond length (2.061 (1) Å) consistent with a bond order greater than 1.

A major area of research in our group is the development of the coordination chemistry of the early transition metals (Ti, V, Cr, Mn) with the thiolate (RS^-) ligand, both because this is an essentially unexplored area and because of the possible occurrence of metal-thiolate (cysteiny) linkages in biological systems containing these metals.¹⁷ For vanadium our efforts to date have concentrated on the V(IV) oxidation level. Remarkably little has been done in this area in the past, except for some studies in which the thiolate group is present as a bi- or polyfunctional ligand, e.g. 2-aminoethanethiol,¹⁸ 2-aminobenzenethiol,¹⁸ and L-cysteine;¹⁹ none of these have been structurally characterized. Our initial studies have been mainly with ethane-1,2-dithiol ($edtH_2$) and they have led to the synthesis of square-pyramidal $[VO(edt)_2]^{2-}$ (**1**).²⁰ Exchange of the oxygen atom for sulfur has also allowed the synthesis of the thiovanadyl complex $[VS(edt)_2]^{2-}$ (**2**). Herein are described the preparations of these two species, together with their crystal structures and a comparison of some of their properties.

Experimental Section

All manipulations were performed with use of standard inert-atmosphere techniques and a purified dinitrogen atmosphere. Solvents were purified by distillation, except for ethanol, which was dried over molecular sieves and degassed before use. Bis(pentane-2,4-dionato)oxovanadium(IV), $VO(acac)_2$, was prepared as described elsewhere²¹ and recrystallized from $CHCl_3$ /acetone. Ethane-1,2-dithiol and hexamethyldisilthiane (Petrarch) were used as received.

A. $(PPh_4)Na[VO(edt)_2]\cdot 2EtOH$. A solution of Na_2edt (45 mmol) in ethanol (100 mL) was prepared from the thiol (3.78 mL, 45 mmol) and Na metal (2.07 g, 90 mmol). Solid $VO(acac)_2$ (2.98 g, 11.3 mmol) was added with stirring; the solid rapidly dissolved, and a deep green solution was generated. Addition of PPh_4Br (9.44 g, 22.5 mmol) and cooling overnight at $-20^\circ C$ led to the formation of green crystals. These were collected by filtration, washed with EtOH and Et_2O , and dried in vacuo. Recrystallization from warm EtOH/ Et_2O yields the analytically pure product in 48% overall yield. Anal. Calcd for $C_{32}H_{40}O_3PS_4NaV$: C, 54.45; H, 5.71; S, 18.17. Found: C, 54.31; H, 5.71; S, 17.97.

$(NMe_4)Na[VO(edt)_2]\cdot 2EtOH$ was prepared similarly with use of NMe_4Cl (2.47 g, 22.5 mmol). After addition of the NMe_4Cl , the solution was filtered to remove precipitated solids (mainly NaCl) and set aside at $-20^\circ C$ for 2–3 days. Large, well-formed diamond-shaped green crystals were obtained, which were collected by filtration, washed with EtOH and Et_2O and dried in vacuo; yield 80%. This material was not analyzed, but a suitable crystal was chosen for a structure determination.

Table I. Crystallographic Data for $(NMe_4)Na[VO(edt)_2]\cdot 2EtOH$ (A) and $(PPh_4)Na[VS(edt)_2]\cdot xEt_2O$ (B)

	A	B
formula	$C_{12}H_{32}NO_3S_4NaV$	$C_{32}H_{38}OPS_5NaV^c$
molar mass	440.56	703.86 ^c
cryst syst	monoclinic	triclinic
space group	$P2_1/n$	$P\bar{1}$
temp, $^\circ C$	-159	-160
a, Å	21.312 (5) ^a	17.201 (5) ^b
b, Å	10.906 (2)	10.983 (3)
c, Å	9.381 (1)	9.919 (3)
α , deg		65.84 (1)
β , deg	92.77 (1)	106.63 (1)
γ , deg		93.32 (2)
Z	4	2
vol, Å ³	2177.86	1634.42
radiation	Mo K α (0.71069 Å)	Mo K α (0.71069 Å)
abs coeff, cm ⁻¹	8.365	6.864
cryst size, mm	$0.23 \times 0.21 \times 0.18$	$0.21 \times 0.21 \times 0.19$
scan speed, deg/min	4.0	4.0
scan width, deg	2.0 + dispersion	2.0 + dispersion
scan range, deg	$6 \leq 2\theta \leq 45$	$6 \leq 2\theta \leq 45$
no. of unique intens	2816	4284
no. of obsd intens	2557 ($F \geq 2.33\sigma(F)$)	3684 ($F \geq 3\sigma(F)$)
R, %	3.46	4.38
R_w , %	4.25	4.87
goodness of fit	1.229	1.224

^a 40 reflections at $-159^\circ C$. ^b 30 reflections at $-160^\circ C$. ^c $x = 1$.

Recrystallization from warm DMF/MeCN yields very thin waferlike crystals.

B. $(PPh_4)Na[VS(edt)_2]\cdot xEt_2O$. A slurry of $(Ph_4P)Na[VO(edt)_2]\cdot 2EtOH$ (2.2 g, 3.1 mmol) in MeCN (40 mL) was treated with hexamethyldisilthiane (0.66 mL, 3.1 mmol). Rapid formation of a deep red-purple color was observed, and all the solid dissolved. On additional stirring, the solution became progressively more orange-brown. The solution was left overnight at ambient temperature and then filtered. Addition of an equal volume of ether followed by storage at $-20^\circ C$ yielded the crude product as brown microcrystals. These were collected by filtration, washed with ether, and dried in vacuo. Recrystallization from MeCN/ Et_2O yielded brown prismatic crystals in 34% overall yield. The presence of ether in the crystal lattice was detected by 1H NMR and X-ray crystallography. An analytical sample dried for several hours in vacuo suggested the absence of solvent molecules. Anal. Calcd for $C_{28}H_{28}PS_5NaV$: C, 53.40; H, 4.48; S, 25.46. Found: C, 53.52; H, 4.80; S, 25.04. The NMe_4^+ salt was prepared similarly on a small scale for IR studies.

Both **1** and **2** are oxygen sensitive, particularly in solution; **2** is much more sensitive than **1**, readily yielding the latter with H_2O or O_2 .

X-ray Crystallography and Structure Solution. Data were collected at approximately $-159^\circ C$; details of the diffractometry, low-temperature facilities, and computational procedures employed by the Molecular Structure Center are available elsewhere.²² Data collection parameters are summarized in Table I. The structures were solved by a combination of direct methods and Fourier techniques and refined by full-matrix least-squares.

$(NMe_4)Na[VO(edt)_2]\cdot 2EtOH$ crystallizes in monoclinic space group $P2_1/n$. The asymmetric unit contains the anion, NMe_4^+ , Na^+ , and two solvent molecules. Refinement proceeded uneventfully with no sign of any disorder problems although one of the solvent molecules had rather large thermal parameters. In the latter stages, hydrogen atoms became clearly visible, except for the aforementioned ethanol. Non-hydrogen atoms were refined anisotropically. In the final full-matrix refinement, anion and NMe_4^+ hydrogen atoms were refined isotropically whereas solvent hydrogen atoms were included as fixed-atom contributors, except for the three methyl hydrogens of the poorly defined ethanol, which were omitted altogether. Final R values are included in Table I.

$(PPh_4)Na[VS(edt)_2]\cdot xEt_2O$ crystallizes in triclinic space group $P\bar{1}$ with the asymmetric unit containing the anion, PPh_4^+ , Na^+ , and ether molecules. Location and refinement of the anion and cations proceeded routinely with no disorder among these atoms. At this stage a difference Fourier revealed numerous peaks belonging to seriously disordered ether molecules in a channel that runs through the lattice. Nine distinct peaks were located and their positions and occupancies refined. Three of the peaks are within reasonable distance of the Na atom (2.38–2.66 Å) and

- (9) (a) Shiro, M.; Fernando, Q. *J. Chem. Soc. D* **1971**, 63; *Anal. Chem.* **1971**, 43, 1212. (b) Pasquali, M.; Marchetti, F.; Floriani, C.; Merlino, S. *J. Chem. Soc., Dalton Trans.* **1977**, 139.
- (10) Mathew, M.; Carty, A. J.; Palenik, G. J. *J. Am. Chem. Soc.* **1970**, 92, 3197.
- (11) Farmer, R. L.; Urbach, F. L. *Inorg. Chem.* **1974**, 13, 587.
- (12) Rice, C. E.; Robinson, W. R.; Tofield, B. E. *Inorg. Chem.* **1976**, 15, 345.
- (13) Goedken, V. L.; Ladd, J. A. *J. Chem. Soc., Chem. Commun.* **1981**, 910.
- (14) Poncet, J. L.; Guillard, R.; Friant, P.; Gouton, J. *Polyhedron* **1983**, 2, 417.
- (15) Callahan, K. P.; Durand, P. J.; Rieger, P. H. *J. Chem. Soc., Chem. Commun.* **1980**, 75. Callahan, K. P.; Durand, P. J. *Inorg. Chem.* **1980**, 19, 3211.
- (16) Sato, M.; Miller, K. M.; Enemark, J. H.; Strouse, C. E.; Callahan, K. P. *Inorg. Chem.* **1981**, 20, 3571.
- (17) For example, a Mn(III)-cysteine bond seems to be occurring in acid phosphatase from the sweet potato: Sugiura, Y.; Kawabe, H.; Tanaka, H.; Fujimoto, S.; Ohara, A. *J. Biol. Chem.* **1981**, 256, 10664.
- (18) (a) Hodge, A.; Nordquest, K.; Blinn, E. L. *Inorg. Chim. Acta* **1972**, 6, 491. (b) Larkworthy, L. F.; Murphy, J. M.; Phillips, D. J. *Inorg. Chem.* **1968**, 7, 1436.
- (19) Sakurai, H.; Hamada, Y.; Shimomura, S.; Yamashita, S. *Inorg. Chim. Acta* **1980**, 46, L119.
- (20) Wiggins, R. W.; Huffman, J. C.; Christou, G. *J. Chem. Soc., Chem. Commun.* **1983**, 1313.
- (21) Rowe, R. A.; Jones, M. M. *Inorg. Synth.* **1957**, 5, 113.

- (22) Huffman, J. C.; Lewis, L. N.; Caulton, K. G. *Inorg. Chem.* **1980**, 19, 2755.

Table II. Fractional Coordinates ($\times 10^4$) of the Non-Hydrogen Atoms in $[\text{VO}(\text{edt})_2]^{2-}$ (1)

atom	x	y	z
V	8748 (1)	131 (1)	243 (1)
O(2)	9347 (1)	76 (2)	-763 (2)
S(3)	8079 (1)	1629 (1)	-869 (1)
C(4)	7837 (2)	700 (3)	-2422 (4)
C(5)	7512 (2)	-458 (4)	-1977 (4)
S(6)	7965 (1)	-1290 (1)	-574 (1)
S(7)	8977 (1)	1639 (1)	2012 (1)
C(8)	9177 (2)	752 (4)	3635 (4)
C(9)	9491 (2)	-440 (3)	3310 (4)
S(10)	8988 (1)	-1348 (1)	2065 (1)
N(11)	8082 (1)	-4889 (2)	1857 (3)
C(12) ^a	7736 (2)	-3718 (4)	2067 (6)
C(13) ^a	8555 (2)	-4718 (4)	751 (5)
C(14) ^a	8411 (2)	-5258 (5)	3234 (5)
C(15) ^a	7626 (2)	-5867 (4)	1397 (5)
Na(16)	5048 (1)	3256 (1)	5063 (1)
O(17)	5809 (1)	2240 (2)	6620 (2)
C(18)	5721 (2)	2601 (4)	8066 (4)
C(19)	6256 (2)	2240 (4)	9053 (4)
O(20)	4381 (1)	1911 (2)	3799 (3)
C(21)	4442 (2)	978 (5)	2757 (5)
C(22)	4503 (4)	1439 (7)	1352 (6)

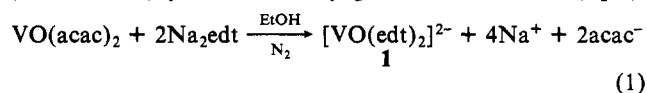
^a Cation methyl carbon atoms.

were assigned as ether oxygens (O(37), O(41), and O(44)). Their occupancies were refined to 0.48, 0.26, and 0.16, respectively. The remaining six peaks were assigned as ether carbon atoms. Only C(39), which sits on the inversion center at $1, \frac{1}{2}, \frac{1}{2}$, has a high occupancy (0.97); the remaining carbons have occupancies in the range 0.51–0.60. There are several ways to connect the nine carbon and oxygen atoms to generate recognizable fragments of the ether molecule; however, many interatomic distances and angles are unreasonable, e.g. several C–C bond lengths > 1.7 Å. As a result, we have not pursued a better model for the disorder problem, and in any case the behavior of the solvent carbons is of little consequence to the main conclusions of this work. Final *R* values were quite satisfactory and are included in Table I.

Other Measurements. Infrared spectra were recorded as Nujol mulls on a Perkin-Elmer Model 283 spectrophotometer. Electronic spectra were obtained in MeCN solution on a Perkin-Elmer Model 330 spectrophotometer. Electrochemical measurements were performed in the cyclic voltammetric mode with an IBM Model EEC 25 voltammetric analyzer in conjunction with a glassy-carbon working electrode, a platinum-wire auxiliary electrode, and an SCE reference electrode. The supporting electrolyte was 0.1 M tetra-*n*-butylammonium perchlorate (TBAP), and concentrations of electroactive species were in the ca. 4 mM range. Measurements were performed in MeCN solution, and potentials are quoted vs. the normal hydrogen electrode (NHE) with ferrocene as an internal standard ($E_{1/2} = 0.400$ V vs. NHE).²³ No *iR* compensation was employed.²³

Results and Discussion

Synthesis. Our initial attempts to prepare vanadium(IV) thiolate complexes involved the reaction of $\text{VO}(\text{acac})_2$ with various amounts of excess PhS^- in EtOH. This approach yielded green solutions, but we found it difficult to isolate a clean product from these systems. Suspecting that the desired ligand exchange was not proceeding to completion, i.e. that mixtures of partially and completely substituted products were being generated, we decided to utilize the more basic alkanethiolates and, as an extra driving force, to employ a bidentate ligand to invoke the chelate effect. The ligand chosen was ethane-1,2-dithiol (edtH_2). Reaction of the sodium salt, Na_2edt , with $\text{VO}(\text{acac})_2$ in a 4:1 molar ratio (100% excess) yielded intensely green solutions of **1** (eq 1).



Addition of excess quaternary ammonium or phosphonium salts yielded the product as a highly crystalline precipitate containing one ammonium (or phosphonium) group, one Na^+ , the anion, and

Table III. Fractional Coordinates ($\times 10^4$) of the Non-Hydrogen Atoms in $[\text{VS}(\text{edt})_2]^{2-}$ (2)

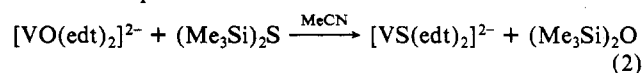
atom	x	y	z
V	8145 (1)	10047 (1)	3633 (1)
S(2)	7000 (1)	9335 (1)	3060 (1)
S(3)	8296 (1)	11878 (1)	1400 (1)
C(4)	8518 (3)	10951 (7)	378 (6)
C(5)	9257 (3)	9986 (7)	1374 (7)
S(6)	9126 (1)	8912 (1)	3243 (2)
S(7)	8125 (1)	11770 (1)	4464 (1)
C(8)	8457 (3)	10984 (7)	6552 (7)
C(9)	8323 (3)	9528 (8)	7167 (6)
S(10)	8757 (1)	8692 (1)	6269 (1)
Na(11)	-309 (1)	1972 (2)	3767 (3)
P(12)	3893 (1)	4272 (1)	2383 (1)
C(13) ^a	3293 (2)	4672 (4)	3379 (4)
C(14)	2689 (2)	3837 (4)	3831 (5)
C(15)	2229 (3)	4120 (4)	4618 (6)
C(16)	2362 (3)	5254 (4)	4921 (5)
C(17)	2953 (3)	6088 (4)	4465 (5)
C(18)	3425 (2)	5806 (4)	3694 (5)
C(19) ^a	3217 (2)	3804 (4)	950 (5)
C(20)	3345 (2)	2614 (4)	860 (5)
C(21)	2798 (3)	2278 (4)	-246 (5)
C(22)	2132 (3)	3121 (5)	-1257 (5)
C(23)	2001 (3)	4304 (5)	-1166 (6)
C(24)	2534 (3)	4646 (5)	9936 (6)
C(25) ^a	4636 (2)	2909 (4)	3673 (5)
C(26)	4647 (2)	2197 (4)	5196 (5)
C(27)	5246 (3)	1181 (4)	6185 (5)
C(28)	5833 (2)	892 (4)	5632 (6)
C(29)	5825 (2)	1585 (4)	4110 (5)
C(30)	5231 (2)	2593 (4)	3124 (5)
C(31) ^a	4435 (2)	5722 (4)	1597 (4)
C(32)	4027 (2)	6884 (4)	371 (5)
C(33)	4428 (3)	8040 (4)	-78 (5)
C(34)	5239 (3)	8057 (4)	693 (5)
C(35)	5650 (2)	6918 (4)	1903 (5)
C(36)	5252 (2)	5751 (4)	2361 (5)
O(37) ^b	7 (6)	4533 (12)	2596 (16)
C(38)	10122 (6)	5341 (11)	3345 (12)
C(39) ^{b,c}	10000	5000	5000
C(40) ^b	86 (8)	5288 (15)	1442 (19)
O(41) ^b	-65 (9)	4112 (15)	3833 (18)
C(42) ^b	369 (13)	6567 (22)	2779 (24)
C(43) ^b	9866 (12)	3278 (20)	-732 (23)
O(44) ^b	9916 (10)	4149 (18)	2078 (22)
C(45) ^b	-17 (36)	5410 (49)	17 (88)

^a Carbon atoms 13, 19, 25, and 31 are bound to the phosphorus; other phenyl carbons are numbered consecutively around the ring.

^b Disordered ether atoms. ^c Position fixed on the inversion center.

two solvent molecules per asymmetric unit.

Conversion of $[\text{VO}(\text{edt})_2]^{2-}$ (**1**) to $[\text{VS}(\text{edt})_2]^{2-}$ (**2**) was achieved with hexamethyldisilthiane, $(\text{Me}_3\text{Si})_2\text{S}$. The efficiency of this reagent in effecting O/S exchange has recently been demonstrated,²⁴ the silicon-containing product being hexamethyldisiloxane, $(\text{Me}_3\text{Si})_2\text{O}$. Treatment of a slurry of $(\text{PPh}_4)\text{Na}[\text{VO}(\text{edt})_2] \cdot 2\text{EtOH}$ in MeCN with $(\text{Me}_3\text{Si})_2\text{S}$ yielded an immediate and intense red-purple coloration,²⁵ which slowly converted to orange-brown on stirring overnight at ambient temperature. Addition of anhydrous diethyl ether yielded orange-brown crystals, which were recrystallized from MeCN/ Et_2O . Establishment of the product as containing the desired dianion $[\text{VS}(\text{edt})_2]^{2-}$ (**2**) was accomplished by X-ray crystallography. Its formation is summarized in eq 2.



Description of Structures. Fractional atomic coordinates for the non-hydrogen atoms of **1** and **2** are listed in Tables II and

(24) Do, Y.; Simhon, E. D.; Holm, R. H. *Inorg. Chem.* **1983**, *22*, 3809.

(25) This intermediate has been isolated and is currently under structural characterization: Money, J. K.; Huffman, J. C.; Christou, G., work in progress.

(23) Gagne, R. G.; Koval, C. A.; Lisensky, G. C. *Inorg. Chem.* **1980**, *19*, 2855.

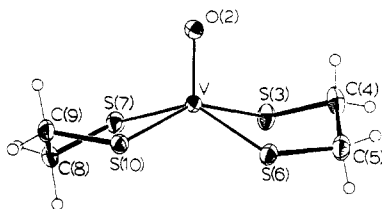


Figure 1. Structure and atom-labeling scheme of anion **1**. Non-hydrogen atoms are depicted as 50% probability ellipsoids; hydrogen atoms are depicted as spheres of arbitrary size.

III, respectively. The structure of **1** is depicted in Figure 1; the structure of **2** is identical except for the presence of $V=S$ instead of $V=O$. The atom-labeling scheme is applicable to both compounds.

The coordination geometry of the vanadium atom in **1** is square pyramidal with the oxygen at the apex. The vanadium is 0.668 Å above the S(3,6,7,10) least-squares plane (maximum deviation by S(6), 0.092 Å). There is no crystallographically imposed symmetry, but **1** closely approximates C_{2v} symmetry and the VOS_4 core C_{4v} symmetry. This is evident from an examination of the V-S bond lengths and S-V-S angles listed in Table IV. The O-V-S angles are in a fairly narrow range (104.0–110.4°), but more noticeable are the S-V-S angles in the range 84.82–86.39°. Thus, there is no differentiation between inter- and intraligand S-V-S angles. The S_4 basal plane is consequently very close to being a perfect square, a fact emphasized by consideration of the S...S and V-S distances in Table IV.

The $V=O$ bond distance (1.625 (2) Å) is quite long for this group in five-coordinate complexes. Most square-pyramidal vanadyl species have $V=O$ bond lengths ≤ 1.6 Å. Bonds greater than 1.60 Å are usually associated with (i) the presence of a sixth ligand trans to the vanadyl oxygen,^{5,7,8} (ii) trigonal-bipyramidal coordination geometry,⁹ or (iii) the presence of $V=O \cdots V=O \cdots$ linear polymers.^{10–12} It is thus tempting to rationalize the relatively long $V=O$ bond of **1** as being due to (i) the greater polarizability of sulfur vs. that of first-row elements (O, N, F) leading to greater covalency in V-S bonds and consequently greater net σ (and π ?) electron density donation to the vanadium and/or (ii) the dianionic nature of the ligands resulting in charge buildup at the vanadium. Both these effects are probably operative, causing reduction in axial oxygen-to-vanadium π donation and a weakening (and lengthening) of the multiple bond. We note, however, that both $VO(dtc)_2$ ($dtc = N,N$ -diethyldithiocarbamate)³ and $[VO(bzil)_2]^{2-}$ ($bzil =$ benzilate dianion) have "normal" $V=O$ bond lengths of 1.591 (4) and 1.584 (11) Å, respectively. Perhaps the safest generalization that should be made regarding a correlation between the $V=O$ bond length and the identity of the basal ligands is that there is no safe generalization to be made. The value of 1.625 (2) Å does not, however, seem to be due to some unique property of the ethane-1,2-dithiolate ligand; $[VO(pdt)_2]^{2-}$ ($pdt =$ propane-1,3-dithiolate) has an identical $V=O$ bond length (1.628 (2) Å).²⁷ The thiolate ligands also have significant effects on other properties of **1** as will be discussed below.

The structure of **2** is essentially identical with that of **1**. Of immediate interest is the $V=S$ bond length, which is 2.087 (1) Å. The major change with respect to **1** is an increase in the distance (0.784 Å) between the vanadium and the S(3,6,7,10) least-squares plane (maximum deviation by S(7), 0.0875 Å). This is 0.116 Å greater than in **1**. As a result the mean E-V-S angle is ca. 3° larger than in **1**, the mean basal S-V-S angle ca. 2° smaller, and the mean diagonal angle ca. 6° smaller. There is also a slight differentiation in the basal angles and S...S distances, interligand values are now noticeably smaller than intraligand values.

Complex **2** represents the second example of a structurally characterized thiovanadyl(2+) species, the other being $VS(acen)$.¹⁶ The structure of $VO(acen)$ is also known, allowing some com-

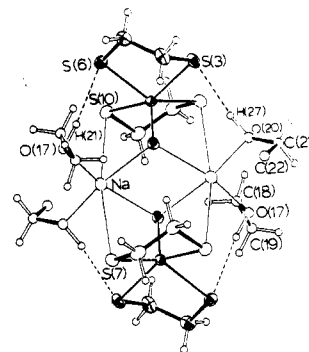


Figure 2. Structure of centrosymmetric $[Na_2[VO(edt)_2]_2 \cdot 4EtOH]^{2-}$ (I) showing hydrogen-bonding interactions. For clarity, only one pair of symmetry-related S and C atoms of the anion are shaded.

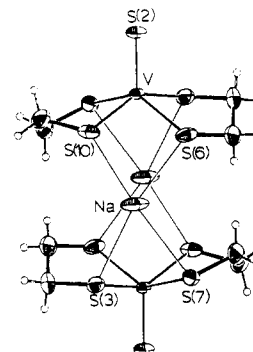


Figure 3. Structure of centrosymmetric $[Na_2[VS(edt)_2]_2 \cdot xEt_2O]^{2-}$ (II). The disordered ether molecules are omitted.

parisons to be made regarding the effect of O/S exchange, with basal ligand constancy. In particular, the change in $V=E$ bond length as one goes from **1** to **2** is 0.462 Å, which compares favorably with 0.476 Å for $VE(acen)$ ($E = O$, 1.585 (7) Å; $E = S$, 2.061 (1) Å). It thus appears that although the basal ligands govern the absolute magnitude of the $V=E$ bond lengths, the change as one goes from $V=O$ to $V=S$ is approximately constant. However, more examples are required to determine the generality of this observation.

Molecular Architecture. The presence of Na^+ ions in both the $E = O$ and $E = S$ complexes lead to extensive $Na \cdots O$ and $Na \cdots S$ interactions in the crystal involving ligand and solvent atoms. The resultant molecular architecture is quite aesthetic and dependent on the identity of E. For both complexes, discrete units are observed rather than an infinite network. Their structures are depicted in Figures 2 and 3; the formulas of the units are $(NMe_4)_2Na_2[VO(edt)_2]_2 \cdot 4EtOH$ (I) and $(PPh_4)_2Na_2[VS(edt)_2]_2 \cdot xEt_2O$ (II).

The structure of I, which possesses idealized C_{2h} symmetry, has each vanadyl oxygen bridging two Na atoms to yield an Na_2O_2 rhomb, at the middle of which is the center of symmetry. The $Na \cdots Na$ length is 3.810 (3) Å, and the mean $Na \cdots O$ distance is 2.448 Å. Each Na^+ also has two trans interactions with thiolate sulfurs S(7) and S(10) from different $VO(edt)_2$ units, and distorted-octahedral coordination is completed by two terminal ethanol molecules. $Na \cdots S$ distances are listed in Table IV; additional data are available as supplementary material. The $V \cdots V$ distance is 5.387 (1) Å. S(3) and S(6) are not involved in $Na \cdots S$ contacts but are H bonded to the ethanol -OH protons. Thus, $S(3) \cdots H(27)$ and $S(6) \cdots H(21)$ are 2.259 and 2.297 Å, respectively, and the corresponding angles $S(3)-H(27)-O(20)$ and $S(6)-H(21)-O(17)$ are 171.3 and 168.8°, respectively. These $H \cdots S$ distances are significantly shorter than the sum of van der Waals radii for H and S (3.05 Å).²⁸

The structure of II has idealized D_{2h} symmetry. In contrast to I, the multiply bonded atom is not involved in interactions with

(26) Chasteen, N. D.; Belford, R. L.; Paul, I. C. *Inorg. Chem.* **1969**, *8*, 408.
(27) Money, J. K.; Huffman, J. C.; Christou, G., unpublished results.

(28) Pauling, L. "The Nature of the Chemical Bond", 3rd ed.; Cornell University Press: Ithaca, NY, 1960; p 260.

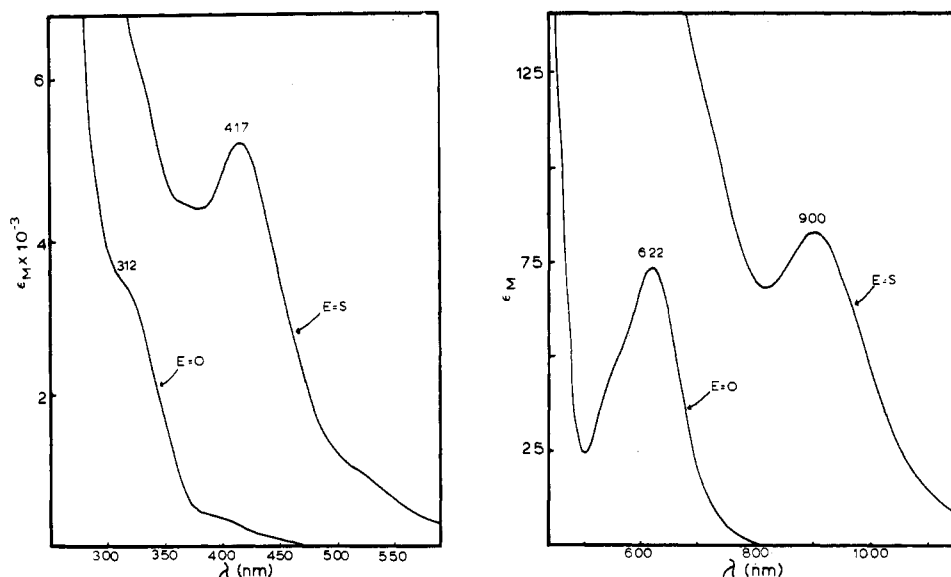


Figure 4. UV-visible absorption spectra of **1** and **2** in MeCN solution.

Table IV. Selected Interatomic Distances (Å) and Angles (deg) in [VE(edt)₂]²⁻ (E = O, S)

	E = O (1)	E = S (2)
V-E(2)	1.625 (2)	2.087 (1)
V-S(3)	2.375 (1)	2.375 (1)
V-S(6)	2.377 (1)	2.359 (1)
V-S(7)	2.371 (1)	2.358 (1)
V-S(10)	2.388 (1)	2.363 (1)
mean	2.378	2.364
Na-S(3)		2.869 (2)
Na-S(6)		2.881 (2)
Na-S(7)	2.995 (2) (2×)	2.941 (2)
Na-S(10)	2.965 (2) (2×)	2.822 (2)
mean	2.980	2.878
E(2)-V-S(3)	104.03 (8)	108.19 (6)
E(2)-V-S(6)	110.36 (8)	110.49 (5)
E(2)-V-S(7)	106.92 (8)	112.87 (5)
E(2)-V-S(10)	104.06 (8)	106.08 (6)
mean	106.34	109.41
S(3)-V-S(6)	84.82 (4)	84.66 (6)
S(7)-V-S(10)	86.39 (4)	85.02 (5)
S(3)-V-S(7)	85.98 (4)	81.52 (6)
S(6)-V-S(10)	85.03 (4)	83.82 (6)
mean	85.56	83.76
S(3)-V-S(10)	151.90 (4)	145.73 (5)
S(6)-V-S(7)	142.72 (4)	136.64 (5)
mean	147.31	141.19
S(3)···S(6) ^a	3.205 (2)	3.188 (2)
S(7)···S(10) ^a	3.257 (2)	3.190 (2)
S(3)···S(7) ^b	3.236 (2)	3.090 (2)
S(6)···S(10) ^b	3.220 (2)	3.154 (2)

^a Intraligand distances. ^b Interligand distances.

the Na⁺ atoms. Instead, the latter are effectively sandwiched between two S(3,6,7,10) basal planes. The Na···Na and V···V distances are 4.032 (3) and 6.168 (1) Å, respectively. The disordered ether molecules (not included) are attached to the Na atoms on the outside of the unit. Na···S distances are listed in Table IV; other data are available in the supplementary material.

The V···S distances in **I** and **II** are essentially identical, the mean value in **I** (2.378 Å) being only slightly longer than in **II** (2.364 Å). The mean Na···S distances show more variation between **I** and **II**, no doubt due to the differing Na environments, being 2.980 and 2.878 Å, respectively; Na···S interactions in the range 2.883–3.106 Å have recently been reported²⁹ for [(Fe₆S₉-

(SMe)₂)₂Na₂]⁶⁻. Such values seem reasonable for predominantly ionic interactions; indeed, the sum of the ionic radii of Na⁺ and S²⁻ is 2.86 Å.

Infrared, Cyclic Voltammetric, and UV/Visible Studies. Infrared spectroscopy has been useful to us as a convenient handle on the extent of O/S substitution and purity of isolated materials. Compounds containing anion **1** show a strong, sharp peak in the 900–1000-cm⁻¹ region usually assigned to the V=O stretch.¹ The exact position of this peak is somewhat dependent on the identity of the cation (no doubt due to solid-state effects), occurring at 930 and 909 cm⁻¹ for the NMe₄⁺ and PPh₄⁺ salts, respectively. Nevertheless, the relatively low values are in accord with the observed lengthening of the V=O bond length. The stretching frequency of the V=S bond in VS(acen) and VS(salen) occurs at 556 and 543 cm⁻¹, respectively.¹⁵ On the basis of these assignments, we anticipated the V=S stretch would be found in the 500–520-cm⁻¹ range. To avoid interference from PPh₄⁺ bands in this region, we employed the NMe₄⁺ salt. On O/S substitution, the band at 930 cm⁻¹ completely disappears and a strong, sharp band at 502 cm⁻¹ appears, which we assign to the V=S stretch. The change in stretching frequencies (428 cm⁻¹) is similar to those for VE(acen) and VE(salen) (E = O, S) on O/S exchange (424 and 439–446 cm⁻¹, respectively), a behavior paralleling changes in V=E bond length.

Neither **1** nor **2** displayed electrochemically reversible behavior when examined by cyclic voltammetry. **1** gave a broad oxidation peak ($E_{pa} = -0.191$ V vs. NHE) with no reduction partner; **2** had a sharper oxidation peak ($E_{pa} = -0.460$ V), but again no corresponding reduction was observed. A very small feature at ca. -0.11 V is also seen on the anodic scan; this is assigned to traces of **1** that may have been an impurity in the sample of **2** employed and/or formed from **2** in the solution from adventitious O₂ or the H₂O in the solvent. A very similar voltammogram has been reported for VS(acen)³⁰ at comparable scan rates (200 mV/s). The oxidation potentials are unusually low. Vanadyl complexes with O/N-based basal ligands usually have oxidation potentials in the range 0.6–1.1 V vs. SCE.^{30,32} With allowance for the different reference electrode employed ($E(\text{SCE}) = +0.24$ V vs. NHE), the potential of **1** is thus shifted to more negative potentials by approximately 1 V. On O/S substitution the potential becomes even more negative, a behavior also seen in the VO(acen)/VS(acen) pair.³⁰ The shift in potential for the latter (0.26 V) is essentially identical with that observed for the 1/2 pair (0.27 V). Again, the basal ligands govern the absolute magnitude of a

(30) Seangprasertkij, R.; Riechel, T. L. *Inorg. Chem.* **1984**, *23*, 991.

(31) Riechel, T. L.; Sawyer, D. T. *Inorg. Chem.* **1975**, *14*, 1869.

(32) Nawi, M. A.; Riechel, T. L. *Inorg. Chem.* **1981**, *20*, 1974.

(29) Strasdeit, M.; Krebs, B.; Henkel, G. *Inorg. Chem.* **1984**, *23*, 1816.

property whereas changes on O/S substitution are essentially constant.

The UV/visible spectra of **1** and **2** in MeCN solution are shown in Figure 4. Pertinent values of λ_{max} (nm) and ϵ_{M} ($\text{L mol}^{-1} \text{cm}^{-1}$) are 312 (sh) (3.6×10^3) and 622 (74) for **1** and 417 (5.4×10^3) and 900 (82) for **2**. The intense, high-energy absorptions are reasonably attributable to charge-transfer transitions and the weaker, low-energy absorptions to essentially metal-based d-d transitions. The major effect of O/S substitution is thus to shift all transitions to lower energy, a behavior also observed in VE(acen) and VE(salen) spectra.¹⁵

Notes

Contribution from the Chemistry Department,
Monash University, Clayton, Victoria 3168, Australia,
and Institute for Inorganic Chemistry,
University of Kiel, 2300 Kiel 1, West Germany

(μ -Oxo)iron(III) Phthalocyanine. Electronic Structure of the Solid Form Obtained from a Dihydroxo-Iron(III) Precursor

Brendan J. Kennedy,[†] Keith S. Murray,^{*†} Peter R. Zwack,[†]
Heinrich Homborg,^{*†} and Winfried Kalz[†]

Received October 12, 1984

The chemistry of iron(III) porphyrins has proved to be of great interest over recent years, both in relation to the biological importance of the heme proteins and because of the large and varied behavior of such systems.¹ The chemistry of the closely related iron(III) phthalocyanines is poorly understood in comparison, partly because it appears that the stable oxidation state of iron phthalocyanines is +2 and partly because the method usually employed to obtain such complexes (the oxidation of $\text{Fe}^{\text{II}}(\text{Pc}(2-))$ under various conditions) often gives rise to a mixture of products.²

It has only been in the last few years that any of the products of oxidation of $\text{Fe}^{\text{II}}(\text{Pc}(2-))$ have been properly characterized, although as yet a crystal structure is available only on (PNP)- $[\text{Fe}^{\text{III}}(\text{Pc}(2-))(\text{CN})_2]$.³ Recently, Ercolani and co-workers⁴ have shown that under suitable conditions the μ -oxo dimer $[\text{Fe}(\text{Pc}(2-))_2\text{O}]$ (**I**) can be isolated. An earlier μ -superoxo formulation for this complex, $[\text{Fe}(\text{Pc}(2-))\text{O}_2\text{Fe}(\text{Pc}(2-))]$ seems to be incorrect.⁵ Ercolani et al.⁴ reported that, depending on the exact reaction conditions used, two crystalline forms of **I** could be isolated, each displaying different IR spectral bands and magnetic susceptibilities. The published magnetic data for these forms of **I**, while suggestive of strong antiferromagnetic coupling between the two iron centers, offered no firm evidence as to the exact size of the coupling. The spin states of the iron centers were likewise not delineated.

Recently, we⁶ have reported alternative syntheses of **I** based on the condensation of the dihydroxo iron(III) complex PNP- $[\text{Fe}(\text{OH})_2(\text{Pc}(2-))]$. The UV-visible and IR spectral data of the samples prepared by these methods correspond exactly to those reported by Ercolani et al. for their sample, μ -oxo **I**. Owing to the unusual reactivity toward molecules such as pyridine and PPh_3 displayed⁷ by μ -oxo **I**, together with the observation⁸ that a monomer such as $\text{Fe}(\text{Pc}(2-))\text{Cl}$ has the relatively rare $S = 5/2$ -³/₂ admixed ground state, it seemed desirable to us to fully characterize the spin-state and electronic properties of $[\text{Fe}(\text{Pc}(2-))_2\text{O}]$.

While the present paper was being reviewed, a study of the Mössbauer spectroscopy of three samples of $[\text{Fe}(\text{Pc}(2-))_2\text{O}]$, prepared by the methods of Ercolani et al., has been reported.⁹ There are some remarkable similarities to the results presented

Acknowledgment. We thank the Research Corp. and the donors of the Petroleum Research Fund, administered by the American Chemical Society, for their generous support of this work and the Bloomington Academic Computing Service for a gift of computer time.

Registry No. **1**, 97689-51-5; **2**, 97689-53-7; $\text{VO}(\text{acac})_2$, 3153-26-2.

Supplementary Material Available: Complete listings of atom coordinates, isotropic and anisotropic thermal parameters, interatomic distances and angles, and calculated and observed structure factors for $(\text{NMe}_4)\text{Na}[\text{VO}(\text{edt})_2] \cdot 2\text{EtOH}$ and $(\text{PPh}_4)\text{Na}[\text{VS}(\text{edt})_2] \cdot x\text{Et}_2\text{O}$ (50 pages). Ordering information is given on any current masthead page.

here, which is intriguing in view of the different methods of synthesis used. The authors do not report any ESR, magnetic or synthetic details on their samples, and this leads them into assignments of minor peaks with which we do not agree. However, this study and the present one both show the existence of only one form of $[\text{Fe}(\text{Pc}(2-))_2\text{O}]$, viz. μ -oxo **I**.

Experimental Section

Abbreviations: PNP = bis(triphenylphosphine)nitrogen(1+); $\text{Pc}(2-)$ = phthalocyaninato dianion.

Synthesis. $[\text{Fe}(\text{Pc}(2-))_2\text{O}]$ was prepared and characterized as described previously.⁶ This involved dissolving 0.57 g (0.5 mmol) of $\text{PNP}[\text{Fe}(\text{OH})_2(\text{Pc}(2-))]$ in dichloromethane, chloroform, or acetone. Within 1 day at room temperature a fine blue crystalline precipitate of $[\text{Fe}(\text{Pc}(2-))_2\text{O}]$ was quantitatively deposited from these solutions. Alternatively, acidification of a saturated solution of $\text{PNP}[\text{Fe}(\text{OH})_2(\text{Pc}(2-))]$ in dichloromethane with acetic acid precipitated the μ -oxo complex immediately. It was also possible to add iodine or water to the dichloromethane solution and obtain the μ -oxo complex. Products were washed with dichloromethane. All attempts to grow single crystals from solution have been unsuccessful. The various samples displayed identical UV-visible and IR spectra.⁶ The IR spectra were also identical with those reported by Ercolani et al.⁴ and by Frampton and Silver⁹ for samples that they label μ -oxo **I**.

Analyses. Microanalytical data were obtained at Kiel University (sample B) and at the Australian Mineral Development Laboratories, Melbourne (sample A (1 year old), sample C). In our experience, there are difficulties in obtaining consistent and reproducible microanalytical data for metal phthalocyanines and metal porphyrins so the results should be treated with some caution. Anal. Calcd for $[\text{Fe}(\text{Pc}(2-))_2\text{O}]$ ($\text{C}_{64}\text{H}_{36}\text{Fe}_2\text{N}_{16}\text{O}$): C, 66.7; H, 2.8. Found, sample A: C, 64.9; H, 2.8; Cl, <0.5. Found, sample B: C, 66.1. Found, sample C: C, 66.6; H, 3.0; Cl, <0.5. All these samples showed the presence of Cl by scanning electron microprobe analysis, presumably due to traces of dichloromethane of solvation being present.

Instrumentation. Mössbauer, ESR and magnetic susceptibility measurements were made as described elsewhere.¹⁰ Double integration of the ESR spectra were carried out with the kind assistance of Dr. J. R. Pilbrow (Department of Physics, Monash University). Electron microprobe analyses were carried out on powdered samples with a Cambridge S410 scanning electron microscope linked via a Nuclear Equipment Corp.

- (1) Scheidt, W. R.; Reed, C. A. *Chem. Rev.* **1981**, *81*, 583.
- (2) Myers, J. F.; Rayner Canham, G. W.; Lever, A. B. P. *Inorg. Chem.* **1975**, *14*, 461.
- (3) (a) Küppers, H.; Homborg, H.; Kalz, W. *Acta Crystallogr.* in press. (b) Kalz, W.; Homborg, H.; Küppers, H.; Kennedy, B. J.; Murray, K. S. *Z. Naturforsch., B: Anorg. Chem., Org. Chem.* **1984**, *39B*, 1478.
- (4) Ercolani, C.; Gardini, M.; Monacelli, F.; Pennesi, G.; Rossi, G. *Inorg. Chem.* **1983**, *22*, 2584.
- (5) Collamati, I. *Inorg. Chim. Acta* **1979**, *35*, L303.
- (6) Kalz, W.; Homborg, H. *Z. Naturforsch., B: Anorg. Chem., Org. Chem.* **1983**, *38B*, 470.
- (7) Ercolani, C.; Gardini, M.; Pennesi, G.; Rossi, G. *J. Chem. Soc., Chem. Commun.* **1983**, 549.
- (8) Kennedy, B. J.; Brain, G.; Murray, K. S. *Inorg. Chim. Acta* **1984**, *81*, L29.
- (9) Frampton, C. S.; Silver, J. *Inorg. Chim. Acta* **1985**, *96*, 187.
- (10) Mitchell, A. J.; Murray, K. S.; Newman, P. J.; Clark, P. E. *Aust. J. Chem.* **1977**, *30*, 2439.

* To whom correspondence should be addressed.

[†] Monash University.

[‡] University of Kiel.